

Spray drying for making Covalent Chemistry: Post-Synthetic Modification of Metal-Organic Frameworks

Luis Garzón-Tovar,[†] Sabina Rodríguez-Hermida,[†] Inhar Imaz,[†] and Daniel Maspoch^{†,‡}*

[†] Catalan Institute of Nanoscience and Nanotechnology (ICN2), CSIC and The Barcelona Institute of Science and Technology, Campus UAB, Bellaterra, 08193 Barcelona, Spain. E-mail: inhar.imaz@icn2.cat, daniel.maspoch@icn2.cat

[‡] ICREA, Pg. Lluís Companys 23, 08010 Barcelona, Spain

ABSTRACT

Covalent post-synthetic modification (PSM) of metal-organic frameworks (MOFs) has attracted much attention due to the possibility to tailor the properties of these porous materials. Schiff-base condensation between an amine and an aldehyde is one of the most common reactions in the PSM of MOFs. Here, we report the use of the spray drying technique to perform this class of organic reactions, either between discrete organic molecules or on the pore surfaces of MOFs, in a very fast (1-2 seconds) and continuous way. Using spray drying, we show the PSM of two MOFs, the amine-terminated UiO-66-NH₂ and the aldehyde-terminated ZIF-90, achieving conversion efficiencies up to 20 % and 42 %, respectively. Moreover, we demonstrate that it can also be used to post-synthetically cross-link the aldehyde groups of ZIF-90 using a diamine molecule with a conversion efficiency of 70 %

INTRODUCTION

Metal-organic frameworks (MOFs), also known as porous coordination polymers (PCPs), have attracted much attention over the past decades due to their potential applications, such as in gas sorption and storage, catalysis, drug delivery and gas separation.¹⁻³ One of the main characteristics of MOFs is the ability to tailor their chemical functionality and/or pore surface chemistry, either by pre- or post-synthetic modification of the organic linker. Covalent post-synthetic modification (PSM) involves an organic reaction carried out on the organic linker while maintaining the MOF integrity.^{4,5}

To date, there are many studies based on the PSM of MOFs involving linkers with different functional groups.⁶⁻⁹ Among them, the most common reaction involves a Schiff-base condensation between an amine and an aldehyde to form an imine *via* water elimination. Using this chemistry, PSM of the 2-aminoterephthalate (NH₂-bdc) linker of UiO-66-NH₂ has been widely studied.¹⁰⁻¹⁶ For example, Lu *et al.* showed the successful PSM of UiO-66-NH₂ with salicylaldehyde (Sal) by heating a mixture of both species in acetonitrile at 40 °C for three days. Once functionalized, they further immobilized Cu(II) salts on the incorporated imine moiety, and used the resulting framework as an efficient catalyst for the aerobic oxidation of alcohols.¹⁰ A similar strategy was also followed to synthesize efficient catalysts for the epoxidation of olefins, the hydrogenation of aromatics, and the reductive amination of aldehydes.^{11,12,13} In these cases, UiO-66-NH₂ was post-synthetically modified with Sal, 2-pyridinecarboxylaldehyde, 4-pyridinecarboxylaldehyde, and 6-((diisopropylamino)methyl)picolinaldehyde followed by the immobilization of Mo(VI) and Ir(I). Also, other amino-terminated MOFs such as IRMOF-3 and Cr-MIL-101-NH₂ have been used for the development of efficient catalysts. Here, both MOFs were first reacted with

“This document is the Accepted Manuscript version of a Published Work that appeared in final form in *Journal of the American Chemical Society*, copyright © American Chemical Society after peer review and technical editing by the publisher. To access the final edited and published work see: <https://doi.org/10.1021/jacs.6b11240>”

pyridine-based aldehydes and then with Cu(I) and Co(II) salts to create heterogeneous catalysts for the synthesis of different 2-aminobenzothiazoles and the aerobic epoxidation of olefins, respectively.^{14,15}

Yaghi *et al.* also reported the use of the Schiff-base condensation reaction to post-synthetically functionalize aldehyde-terminated MOFs. They reacted ZIF-90 with ethanolamine yielding the imine-derivative non-porous ZIF-92.¹⁷ Following the same type of chemistry, ZIF-90 was recently labelled with an Alexa Fluor dye,¹⁸ whereas a mixed ZIF-8-90 sample was post-functionalized with ethylenediamine. This latter PSM allowed the introduction of an aliphatic amine-terminated group to ZIF-8-90, enhancing its CO₂ sorption capacity.¹⁹ In a more recent study, a superhydrophobic ZIF-90 exhibiting a water contact angle value of around 152° was prepared by reacting it with a polyfluorinated amine.²⁰

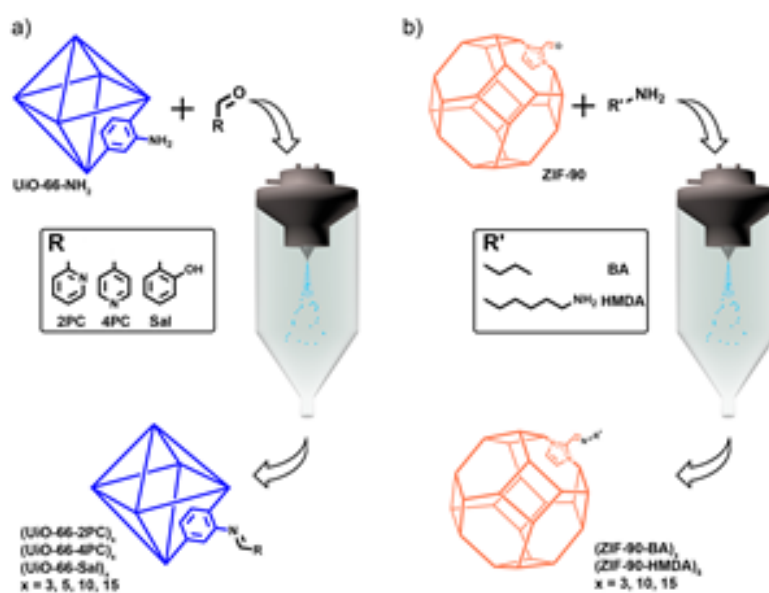
In general, the synthetic conditions for the PSM of MOFs require long reaction times (from 1 to 3 days) and high temperatures. To overcome these limitations, some advances have been done on developing alternative methods for the PSM of MOFs. One of them is based on the PSM of IRMOF-3 and UiO-66-NH₂ by vapour diffusion.²¹ This method allowed the PSM of both MOFs with high conversion rates after heating the solvent-free MOFs with the corresponding aldehyde at 100-120 °C using a vacuum system for 16 h.

Recently, it has been demonstrated that the spray drying (SD) technique is a useful, continuous and scalable method to assemble metal ions and organic ligands to synthesize MOFs.^{22,23} This method allowed to drastically reduce the reaction times down to the second regime, without affecting the properties of the SD-synthesized MOFs. It also enables obtaining them in the form of dried powders and to recycle the solvent used during the fabrication. Here, we extended the use of SD to covalent organic reactions based on the Schiff-base condensation reaction aiming

“This document is the Accepted Manuscript version of a Published Work that appeared in final form in *Journal of the American Chemical Society*, copyright © American Chemical Society after peer review and technical editing by the publisher. To access the final edited and published work see: <https://doi.org/10.1021/jacs.6b11240>”

to be able to post-synthetically modify MOF crystals. UiO-66-NH₂ and ZIF-90 were selected as the target MOFs due to the uncoordinated and available amine and aldehyde groups within their structures, respectively (Scheme 1).

Scheme 1. Illustration of the covalent PSM performed in a) UiO-66-NH₂ and b) ZIF-90 under SD conditions



EXPERIMENTAL SECTION

General procedure for synthesis of imine ligands

In a typical synthesis, a suspension of NH₂-bdc and the corresponding aldehyde (4PC, 2PC and Sal) in 15 mL of ethanol was spray-dried at an inlet temperature of 130 °C, feed rate of 3.0 mL min⁻¹ and a flow rate of 336 mL min⁻¹ using a Mini Spray Dryer B-290 (BUCHI Labortechnik; spray cap: 0.5-mm-hole). The collected solids were characterized by EA, ESI-MS, and ¹H- and ¹³C-NMR spectroscopy. Full experimental details and characterization can be found in the Supporting Information.

“This document is the Accepted Manuscript version of a Published Work that appeared in final form in *Journal of the American Chemical Society*, copyright © American Chemical Society after peer review and technical editing by the publisher. To access the final edited and published work see: <https://doi.org/10.1021/jacs.6b11240>”

Synthesis of UiO-66-NH₂.

UiO-66-NH₂ was synthesized through the previously reported method.²⁸ In a typical synthesis, 35 mL of HCl 37% was added to a solution 0.1 M of ZrCl₄ and 0.1 M of NH₂-bdc in 500 mL of DMF. The resulting mixture was heated at 120 °C under stirring for 2 h. The obtained solid was collected by centrifugation, washed two times with 100 mL of DMF for 12 h at 120 °C, three times with 100 mL of absolute ethanol for 12 h at 60 °C. Finally, the resulting powder was dried at 85 °C overnight (yield = 75 %). Characterization details can be found in the Supporting Information.

Synthesis of ZIF-90.

ZIF-90 was synthesized through the previously reported method.¹⁸ In a typical synthesis, 0.27 mL of trimethylamine (1.96 mmol) was added to a solution 0.01 M of imidazole-2-carboxaldehyde and 3.75 mM of Zn(NO₃)₂·6H₂O in 200 mL of DMF. The resulting mixture was stirred for 1 min at room temperature and then, 100 mL of ethanol was added. The particles were collected by centrifugation, washed five times with ethanol and one time with acetone, and finally dried at 85 °C overnight (yield = 70 %). Characterization details can be found in the Supporting Information.

General synthesis of the PSM of UiO-66-NH₂.

0.150 g of UiO-66-NH₂ (0.085 mmol) was suspended in ethanol (15 mL) and the corresponding aldehyde (4PC, 2PC and Sal) was added to the dispersion. The resulting reaction mixture was then spray-dried at an inlet temperature of 130 °C, feed rate of 3.0 mL min⁻¹ and a flow rate of 336 mL min⁻¹ using a Mini Spray Dryer B-290 (BUCHI Labortechnik; spray cap: 0.5-mm-hole). A yellow powder was collected after 5 min. The resulting solid was then dispersed in 20

“This document is the Accepted Manuscript version of a Published Work that appeared in final form in *Journal of the American Chemical Society*, copyright © American Chemical Society after peer review and technical editing by the publisher. To access the final edited and published work see: <https://doi.org/10.1021/jacs.6b11240>”

mL of ethanol and precipitated by centrifugation. This process was repeated four times. The final product was washed one time with acetone and dried for 12 h at 85 °C. In addition, as a control experiment, the above-mentioned method was reproduced, except that instead of spray drying the reaction mixture, we heated it at 130 °C for 5 min. Under these conditions, a conversion rate of only 3 % was found. Full experimental and characterization details can be found in the Supporting Information.

General synthesis of the PSM of ZIF-90.

A dispersion of ZIF-90 (0.100 g, 0.39 mmol) and the corresponding amine in 15 mL of ethanol was spray-dried at an inlet temperature of 130 °C, feed rate of 3.0 mL min⁻¹ and a flow rate of 336 mL min⁻¹ using a Mini Spray Dryer B-290 (BUCHI Labortechnik; spray cap: 0.5-mm-hole). A yellow powder was collected after 5 min. The resulting solid was then dispersed in 20 mL of ethanol and precipitated by centrifugation. This process was repeated five times. The final product was washed one time with acetone and dried for 12 h at 85 °C. In addition, as a control experiment, the above-mentioned method was reproduced, except that instead of spray drying the reaction mixture, we heated it at 130 °C for 5 min. Under these conditions, the conversion rate was 0 %. Full experimental and characterization details are reported in the Supporting Information.

Quantification protocol.

Samples were digested in strong acidic conditions and their ¹H-NMR spectra were collected to calculate the conversion of imine by the comparison of the integration of the characteristic signals of the corresponding reactants (amine and aldehyde). For the PSM of UiO-66-NH₂, 10 mg of activated sample, 0.6 mL of DMSO-d₆ and 120 μL of HF 5 % were poured in a plastic

“This document is the Accepted Manuscript version of a Published Work that appeared in final form in *Journal of the American Chemical Society*, copyright © American Chemical Society after peer review and technical editing by the publisher. To access the final edited and published work see: <https://doi.org/10.1021/jacs.6b11240>”

NMR tube, and the mixture was sonicated for 1 h until a clear solution was obtained. For the PSM of ZIF-90, 10 mg of sample was digested with 20 μL of DCl and 0.75 mL of DMSO- d_6 .

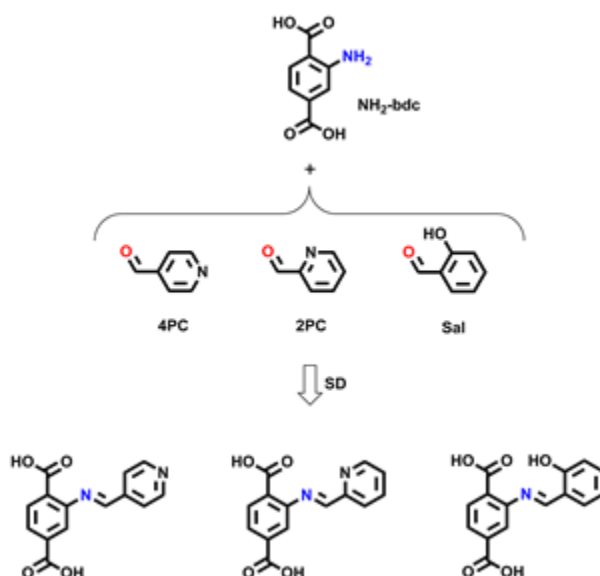
RESULTS & DISCUSSION

Organic Schiff-base condensation reactions conducted *via* spray-drying. To demonstrate that organic reactions and, in particular, Schiff-base condensation reactions between aldehydes and amines could be performed using the SD technique, we initially tested the formation of 2-((pyridin-4-ylmethylene)amino)terephthalic acid using $\text{NH}_2\text{-bdc}$ and 4-pyridinecarboxylaldehyde (4PC) as reactants (Scheme 2). This synthesis started with the mixture of $\text{NH}_2\text{-bdc}$ and 4PC in ethanol (15 mL) at room temperature. The $\text{NH}_2\text{-bdc}$:4PC molar ratio was systematically changed from 1:1, 1:2 and 1:3. Each suspension was then spray-dried at a feed rate of 3.0 mL min^{-1} and an inlet temperature of 130 $^\circ\text{C}$, using a Mini Spray Dryer B-290. This inlet temperature was selected to assure the evaporation of ethanol as well as to force the evaporation of the water formed during the Schiff-base condensation reaction. For each reaction, a yellow powder was collected after 5 min. $^1\text{H-NMR}$ spectra of all collected powders confirmed the imine formation by the appearance of a peak at 8.17 ppm corresponding to the imine proton (Figures 1a, S1). The synthesis of 2-((pyridin-4-ylmethylene)amino)terephthalic acid was further corroborated by $^{13}\text{C-NMR}$ (peak corresponding to the carbon atom of the CH=N imine group at 163 ppm; Figures 1b, S2) and ESI-MS (calculated for $[\text{M-H}]^-$ $[\text{C}_{14}\text{H}_9\text{N}_2\text{O}_4]$: $m/z = 269.0568$; found $m/z = 269.0566$; Figure S3). We finally determined the conversion rate of each reaction by comparing the integration of the peaks at 8.17 ppm (imine proton) and at 7.02 ppm (aromatic proton of the unreacted $\text{NH}_2\text{-bdc}$). The conversion rates were 37 %, 84 % and 92 % for the $\text{NH}_2\text{-bdc}$:4PC molar ratios of 1:1, 1:2 and 1:3, respectively

“This document is the Accepted Manuscript version of a Published Work that appeared in final form in *Journal of the American Chemical Society*, copyright © American Chemical Society after peer review and technical editing by the publisher. To access the final edited and published work see: <https://doi.org/10.1021/jacs.6b11240>”

We then extended the SD synthesis to two other imine compounds (Scheme 2). The syntheses were done using the same conditions as for 2-((pyridin-4-ylmethylene)amino)terephthalic acid, except that instead of 4PC, we used 2-pyridinecarboxylaldehyde (2PC; conversion rate: 87 %) and Sal (conversion rate: 75 %) in a NH₂-bdc:2PC/Sal molar ratio of 1:3. In both cases, the expected imine compounds were successfully synthesized, as confirmed by ¹H- and ¹³C-NMR and ESI-MS (Figures S4-S9).

Scheme 2. Imine molecules synthesized *via* SD.



The high conversion rates obtained in these Schiff-base condensation reactions are remarkable if we consider that, to the best of our knowledge, this is the first time that discrete organic molecules have been synthesized *via* SD. It is well known that, in these condensation reactions, water is produced so that its removal favours the formation of imines following the Le Chatelier's principle. Since SD is based on the fast evaporation of the liquid, we reason that

water can be rapidly removed from the atomized droplets during the Schiff-base reaction, thereby favouring the formation of the imine bond.

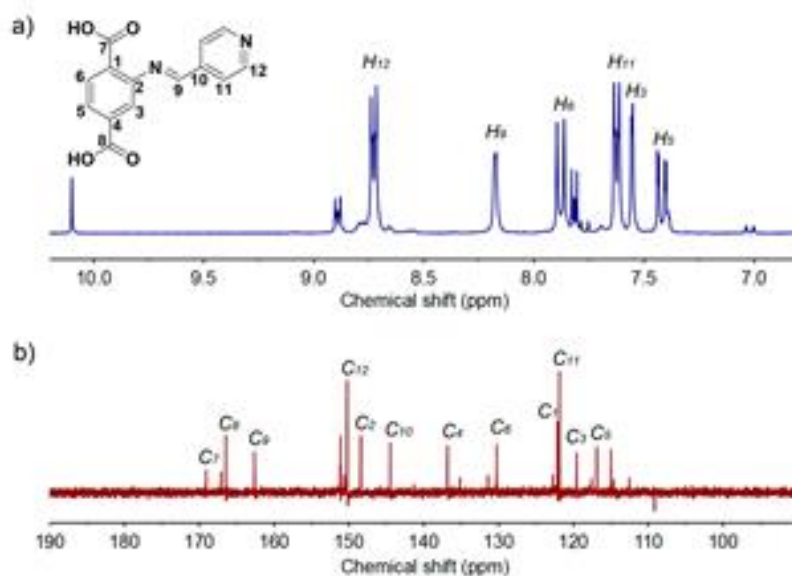


Figure 1. a) ¹H-NMR and b) ¹³C-NMR spectra, collected in DMSO-d₆, of 2-((pyridin-4-ylmethylene)amino)terephthalic acid synthesized using a NH₂-bdc:4PC molar ratio of 1:3. Only the peaks corresponding to the imine molecule are shown.

PSM of UiO-66-NH₂. Once we proved the SD synthesis of imine compounds *via* Schiff-base condensation, we then transferred the same type of chemistry to MOF crystals. For this, we selected UiO-66-NH₂ as the first test case scenario because the amino groups of the NH₂-bdc linkers are pointing into the pores, and of its high chemical and thermal stability.

A series of ethanolic colloidal suspensions (15 mL) containing UiO-66-NH₂ [synthesized under solvothermal conditions; particle size = 245 ± 65 nm; obtained as pure phase as confirmed by X-ray powder diffraction (XRPD), scanning electron microscopy (SEM), N₂ sorption isotherm (S_{BET} = 914 m² g⁻¹) and ¹³C MAS-NMR; see Figures S10-S12] and the aldehydes 4PC, 2PC

“This document is the Accepted Manuscript version of a Published Work that appeared in final form in *Journal of the American Chemical Society*, copyright © American Chemical Society after peer review and technical editing by the publisher. To access the final edited and published work see: <https://doi.org/10.1021/jacs.6b11240>”

and Sal were initially prepared at molar ratios of NH₂-bdc:aldehyde corresponding to 1:3, 1:5, 1:10 and 1:15. Each suspension was then spray-dried under the same conditions as for the pure condensation SD reactions. Once the suspensions had atomized, the different yellow powders were collected from the spray dryer collector, cleaned with ethanol four times and once with acetone, and finally dried at 85 °C for 12 h. The different samples were named as (UiO-66-4PC)_x, (UiO-66-2PC)_x and (UiO-66-Sal)_x (where x is 3, 5, 10 and 15, depending on the equivalents of aldehyde used). Field-emission scanning electron microscopy (FESEM) of all dried powders revealed that initial size and morphology of the parent UiO-66-NH₂ crystals did not change during the SD process (Figure S13). XRPD indicated that all crystalline powders retain the crystallinity of the parent UiO-66-NH₂ MOF (Figures 2b, S14-S16).

To confirm the PSM of UiO-66-NH₂ with the different aldehydes, we first performed ¹³C MAS-NMR on (UiO-66-2PC)₁₅, (UiO-66-4PC)₁₅ and (UiO-66-Sal)₁₅ (Figures 2a, S17-S19). All spectra showed the appearance of a new signal centred at 160-161 ppm, which was attributed to the carbon atom of the CH=N imine group. This peak is consistent with the one observed at 160-162 ppm in the ¹³C-NMR spectra of the imine compounds previously synthesized *via* SD (Figures S2, S5 and S8). It is also in agreement with the ¹³C MAS-NMR signal associated to the imine carbon in other reported post-functionalized UiOs.^{11,12}

The degree of post-synthetic conversion was analysed by first digesting the samples and then analysing the resulting solutions by ¹H-NMR. From the digestion under acidic conditions, the MOF framework is destroyed and the released imine molecules are hydrolysed forming the NH₂-bdc and the corresponding aldehyde. We then calculated the conversion rate by comparison of the integration of one peak at 7.36 ppm corresponding to NH₂-bdc and those peaks at 7.98, 8.52 and 7.52 ppm corresponding to 4PC, 2PC and Sal, respectively (Figures

“This document is the Accepted Manuscript version of a Published Work that appeared in final form in *Journal of the American Chemical Society*, copyright © American Chemical Society after peer review and technical editing by the publisher. To access the final edited and published work see: <https://doi.org/10.1021/jacs.6b11240>”

S20-S32). Also note here that all samples were previously washed three times with ethanol and acetone, and then dried at 85 °C overnight before their digestion. This activation process ensures the removal of all non-reacted aldehyde molecules adsorbed in the pores of the MOFs during the SD process, as confirmed by FT-IR (Figures S33-S35). Table 1 lists the degrees of conversion calculated for all synthesized samples. From this data, it was clear that the degree of conversion increases while increasing the equivalents of aldehyde used in the reaction. For example, the degree of conversion increased from 13 % to 20 % between (UiO-66-2PC)₃ and (UiO-66-2PC)₁₅. It is important to highlight here that the degree of conversion achieved by SD are higher than the ones reported for the PSM of UiO-66-NH₂ with the same aromatic aldehydes.^{10,13} The only exception was the conversion rate of 29 % reported by Bokhoven and co-workers for the formation of (UiO-66-Sal) *via* the vapour-phase method.²¹ However, this latter method is a non-continuous method, which requires vacuum and 16 h to achieve this conversion rate.

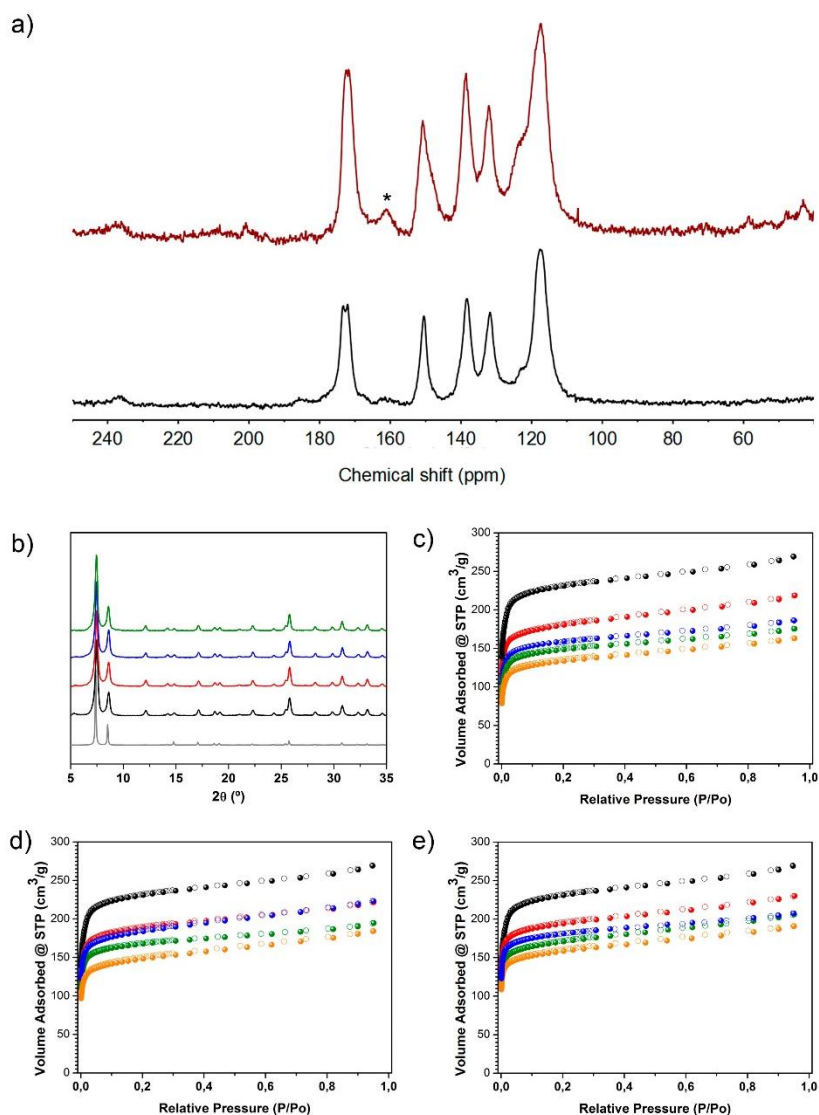


Figure 2. a) ^{13}C MAS-NMR spectra of $(\text{UiO-66-2PC})_{15}$ (red) and UiO-66-NH_2 (black). The signal of CH=N imine group is highlighted with an asterisk (*). b) XRPD patterns of simulated UiO-66-NH_2 (grey) and activated UiO-66-NH_2 (black), $(\text{UiO-66-2PC})_{15}$ (red), $(\text{UiO-66-4PC})_{15}$ (blue) and $(\text{UiO-66-Sal})_{15}$ (green). c-e) N_2 sorption isotherms of (c) $(\text{UiO-66-2PC})_x$, (d) $(\text{UiO-66-4PC})_x$, and (e) $(\text{UiO-66-Sal})_x$ synthesized with different equivalents of aldehyde (x). In c-e, x = 3 (red), x = 5 (blue), x = 10 (green), x = 15 (orange). For comparison, N_2 sorption isotherms of activated UiO-66-NH_2 (black) are also included.

N₂-sorption isotherms were finally measured at 77 K on all activated samples that were further degassed at 200 °C for 12 h under vacuum. We found that the surface area and pore volumes decreased for the samples showing higher degree of conversion (Table 1, Figures 2c-e, S36-S47). We attributed this trend to the fact that the new imine moieties grafted on the pores are bulkier than the amino group.

Table 1. BET areas, pore volumes and % of conversion of UiO-66-NH₂, (UiO-66-2PC)_x, (UiO-66-4PC)_x and (UiO-66-Sal)_x.

MOF	x	S _{BET} (m ² g ⁻¹)	Pore vol. (cm ³ g ⁻¹) ^a	Conversion (%) ^b
UiO-66-NH ₂	--	914	0.3729	--
(UiO-66-2PC) _x	3	699	0.2954	13
	5	625	0.2576	16
	10	586	0.2412	17
	15	516	0.2190	20
(UiO-66-4PC) _x	3	736	0.3056	9
	5	712	0.3015	16
	10	621	0.2652	18
	15	573	0.2441	20
(UiO-66-Sal) _x	3	761	0.3151	11
	5	709	0.2923	14
	10	665	0.2789	16
	15	616	0.2587	19

^a Calculated at P/P₀ ≈ 0.4. ^b Calculated from ¹H-NMR spectra of the digested samples.

PSM of ZIF-90. To explore the versatility of the PSM *via* SD, we then switched to a terminal aldehyde-containing MOF to post-functionalize it with amine molecules. To this end, we selected ZIF-90 that is built up from imidazole-2-carboxaldehyde (ICA) and Zn(II) ions, giving rise to a **sod**-3D porous network showing a pore size around 11 Å and a pore size window around 3.5 Å. Following a similar synthetic procedure as for the PSM of UiO-66-NH₂, three ethanolic suspensions of ZIF-90 [synthesized at room temperature; particle size = 41 ± 9 nm; obtained as pure phase as confirmed by XRPD, SEM, N₂ sorption isotherm (S_{BET} = 1070 m² g⁻¹)

“This document is the Accepted Manuscript version of a Published Work that appeared in final form in *Journal of the American Chemical Society*, copyright © American Chemical Society after peer review and technical editing by the publisher. To access the final edited and published work see: <https://doi.org/10.1021/jacs.6b11240>”

¹) and ¹³C MAS-NMR; see Figure S48-S50] and butylamine (BA) were initially prepared at molar ratios of ICA:BA corresponding to 1:3, 1:10 and 1:15. Each suspension was then spray-dried under the same above-mentioned conditions. Once the suspensions had atomized, the different pale yellow powders were collected from the spray dryer collector, cleaned with ethanol five times and once with acetone, and finally dried at 85 °C for 12 h. Again, the resulting powders were named as (ZIF-90-BA)_x, where x is the number of equivalents of BA.

Similarly, FESEM revealed that initial size and morphology of the parent ZIF-90 crystals did not change during the SD process (Figure S51), whereas XRPD indicated that all crystalline powders retain the parent **sof** structure (Figures 3b, S52). In this case, the formation of imidazol-2-butylmethanimine (IBI) was initially confirmed by FT-IR spectroscopy. Two sets of new bands appeared in the IR spectra of the post-synthetic functionalized ZIF-90 (Figure 3c): 1) the band corresponding to the C=N group, centred at $\approx 1644\text{ cm}^{-1}$, which intensity increased as the equivalents of BA were increased; and 2) the aliphatic C-H stretching of the butyl moiety within the 3000-2700 cm^{-1} range. Moreover, no band corresponding to $-\text{NH}_2$ was observed, indicating that there was not unreacted BA inside the pores of ZIF-90. The formation of IBI was further corroborated by the peaks observed in the ¹³C MAS-NMR spectra at 59, 32, 20 and 13 ppm, which were all attributed to the butyl chain (Figure 3d). The peak at 59 ppm was assigned to the methylene group bonded to imine nitrogen. Moreover, the signal of the aldehyde group was observed at 195 ppm, indicating that not all carbonyl groups were reacted. Finally, the formation of IBI was undoubtedly confirmed by identifying it in the solution resulting from dissolving all (ZIF-90-BA)_x samples using acetic acid (Figures S53-55). Indeed, ¹H-NMR spectra showed peaks at 8.55 and 3.82 ppm that were attributed to the CH=N imine proton and the N-CH₂ methylene protons of IBI, respectively. On the other hand, the peak at $m/z = 152.1180$ in the ESI-MS spectra, matches with the molecular formula of the protonated

IBI [$C_8H_{13}N_3$] $^+$ ($m/z = 152.1182$). Note here that, under these conditions, IBI was also partially hydrolysed.

In order to quantify the conversion rate, 1H -NMR spectra of the digested samples in DCl, DMSO- d_6 were collected (Figure S56-S59). Under these stronger acidic conditions, ZIF-90 is dissolved and the released IBI is completely hydrolysed forming ICA and BA. Thus, the degree of conversion was measured by comparison of the integration of the peaks at 7.57 and 0.86 ppm corresponding to ICA and BA, respectively. We found that the conversion rates were 25 % for (ZIF-90-BA) $_3$, 32 % for (ZIF-90-BA) $_{10}$ and 42 % for and (ZIF-90-BA) $_{15}$.

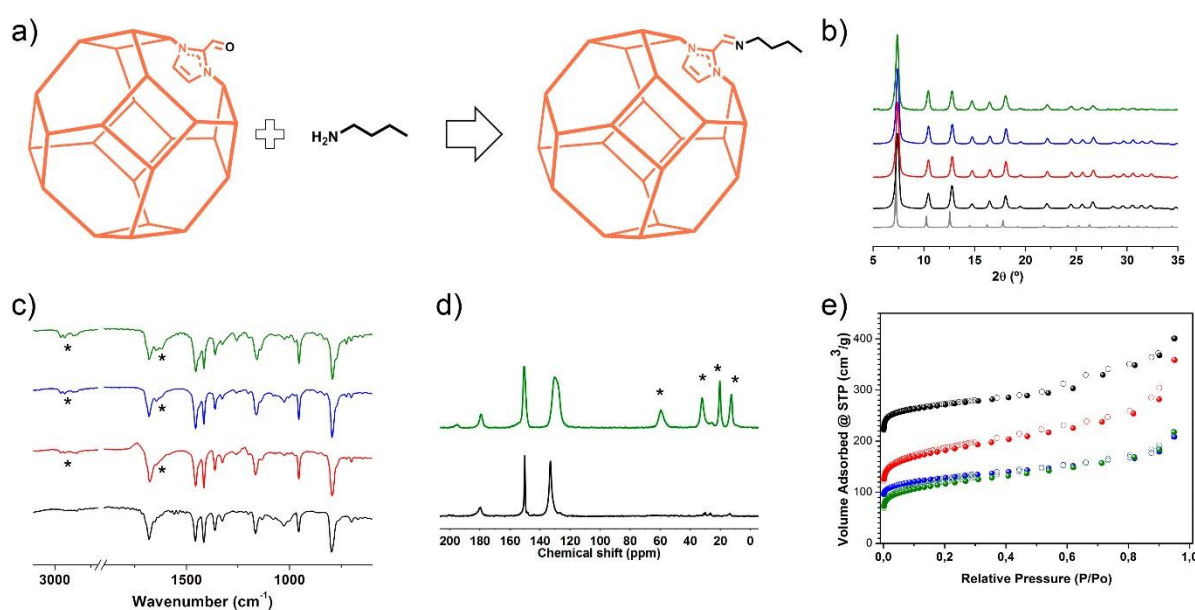


Figure 3. a) Schematic representation of the PSM of ZIF-90 with butylamine *via* SD. b) XRPD patterns of ZIF-90 and (ZIF-90-BA) $_x$, as compared to the simulated powder pattern for the crystal structure of ZIF-90 (grey). c) IR spectra of ZIF-90 and (ZIF-90-BA) $_x$, highlighting the aliphatic C-H and imine C=N vibrational bands with an asterisk (*). d) ^{13}C MAS-NMR spectra of ZIF-90 and (ZIF-90-BA) $_{15}$, where the peaks corresponding to the butyl chains are

highlighted with an asterisk (*). e) N₂ sorption isotherms at 77 K of ZIF-90 and (ZIF-90-BA)_x.

In b-e), ZIF-90 (black), (ZIF-90-BA)₃ (red), (ZIF-90-BA)₁₀ (blue), and (ZIF-90-BA)₁₅ (green).

These results were consistent with the gradual decrease of the S_{BET} values (determined by the N₂-sorption isotherms at 77 K) as the conversion rate (introduction of more bulky butyl chains) was also increased (Figures 3e, S60-S62). The calculated S_{BET} were 670, 483 and 424 m² g⁻¹ for (ZIF-90-BA)₃, (ZIF-90-BA)₁₀, and (ZIF-90-BA)₁₅, respectively. These values corresponded to a loss of 39 %, 45 % and 63 % of the S_{BET} of the parent ZIF-90.

Table 2. BET areas, pore volumes and % of conversion of ZIF-90, (ZIF-90-BA)_x and (ZIF-90-HMDA)₅

MOF	x	S _{BET} (m ² g ⁻¹)	Pore vol. (cm ³ g ⁻¹) ^a	Conver. (%) ^b
ZIF-90		1070	0.4412	---
(ZIF-90-BA) _x	3	670	0.3150	25
	10	483	0.2166	32
	15	424	0.2042	42
(ZIF-90-HMDA) ₅	5	69	0.0377	70

^a Calculated at P/P₀ ≈ 0.4. ^b Calculated from ¹H-NMR spectra of the digested samples.

Previous studies have shown that the introduction of alkyl chains in the pore surfaces of a MOF increases its hydrophobicity.^{24,25} We therefore studied the surface wettability of all post-functionalized ZIF-90 samples by measuring the contact angle (Θ_c) on pressed pellet disks of ZIF-90, (ZIF-90-BA)₃, (ZIF-90-BA)₁₀, and (ZIF-90-BA)₁₅. The Θ_c in each case was 90.4°, 93.3°, 96.1° and 99.3°, respectively - confirming an increase in the hydrophobicity when the conversion rate increases (Figure S63).

“This document is the Accepted Manuscript version of a Published Work that appeared in final form in *Journal of the American Chemical Society*, copyright © American Chemical Society after peer review and technical editing by the publisher. To access the final edited and published work see: <https://doi.org/10.1021/jacs.6b11240>”

Finally, the effect of the particle size on this spray-drying solid/liquid reaction was studied. To this end, a suspension containing larger ZIF-90 crystals (particle size: $18 \pm 9 \mu\text{m}$, Figures S64-S65) and ICA (using ICA:BA 1:15 molar ratio) were spray-dried under the same experimental conditions as described above, *vide supra*. Here, a conversion rate of 22 % was determined by analysing the $^1\text{H-NMR}$ spectra of the digested sample (Figure S66). This value is lower than the one obtained when ZIF-90 nanoparticles were used (42 %), and it is comparable to other conversion rates found in aldehyde-terminated ZIF particles of similar size.^{25,26}

PSM of ZIF-90 with a diamine molecule. We further evaluated the PSM *via* SD by using hexamethylenediamine (HMDA) to crosslink nearby aldehyde groups located on the pores of ZIF-90 (Figure 4a). It is important to mention here that PSM of ZIFs with terminal and aliphatic diamine molecules, such as ethylenediamine, have already been reported. For example, Balkus and co-workers cross-linked neighbouring SIM-1 crystals with ethylenediamine to form a highly compact selective water/methanol membrane.²⁷

Following the procedure applied in the previous PSMs *via* SD, an ethanolic suspension of ZIF-90 and HMDA (molar ratio aldehyde:amine = 1:5) was spray-dried under the same above-mentioned conditions. The collected powder called (ZIF-90-HMDA)₅ was also cleaned with ethanol five times and once with acetone, and dried at 85 °C for 12 h. Again, we did not observe any significant change on the crystal size and morphology during the SD process (Figure S64), and the XRPD indicated that the collected crystals retain the parent ZIF-90 structure (Figure S65).

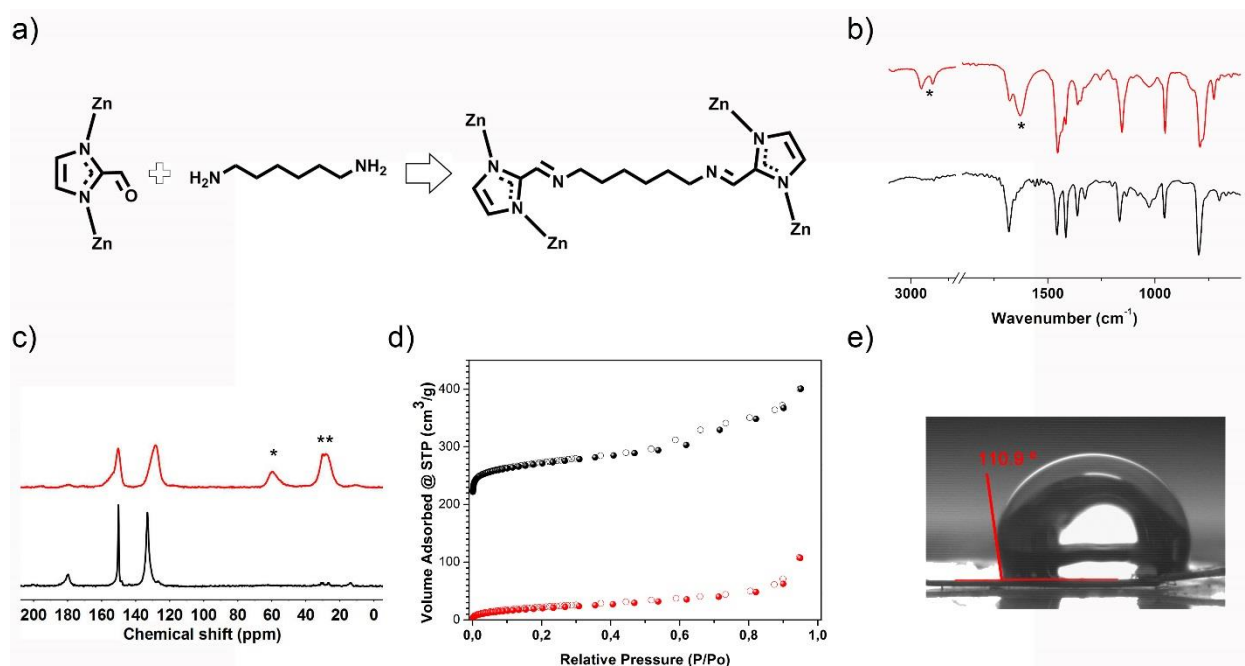


Figure 4. a) Schematic representation of the PSM of ZIF-90 with hexamethylenediamine. b) IR spectra of ZIF-90 (black) and (ZIF-90-HMDA)₅ (red), highlighting the aliphatic C-H and imine C=N vibrational bands with an asterisk (*). c) ¹³C MAS-NMR spectra of ZIF-90 (black) and (ZIF-90-HMDA)₅ (red), where the peaks at the alkyl region are highlighted with an asterisk (*). d) N₂ sorption isotherms of ZIF-90 (black) and (ZIF-90-HMDA)₅ (red). (e) Contact angle image of a pressed pellet disk of (ZIF-90-HMDA)₅.

The FT-IR spectrum of (ZIF-90-HMDA)₅ showed the presence of the characteristic C-H stretching bands of the hexamethyl chains at 2930 and 2850 cm⁻¹ as well as a new band centred at 1630 cm⁻¹ corresponding to the C=N group (Figure 4b). Moreover, the absence of the characteristic vibrational bands of the NH₂ groups suggested that both amino groups of the HMDA were reacted. Altogether these observations agree well with an effective crosslinking of the aldehyde groups located on the pores of ZIF-90 using HMDA.

We further studied this crosslinking by ¹³C MAS-NMR. The spectrum of (ZIF-90-HMDA)₅ showed a low intensity of the peak at 179 ppm corresponding to the aldehyde group, suggesting

“This document is the Accepted Manuscript version of a Published Work that appeared in final form in *Journal of the American Chemical Society*, copyright © American Chemical Society after peer review and technical editing by the publisher. To access the final edited and published work see: <https://doi.org/10.1021/jacs.6b11240>”

a low concentration of this group within the framework (Figure 4c). This result agrees well with the FT-IR spectrum, in which a low intensity of the band at 1675 cm^{-1} corresponding to the aldehyde group was also observed (Figure 4b). On the other hand, three signals in the alkyl-region (60, 30 and 27 ppm) were observed, indicating high symmetry in $(\text{ZIF-90-HMDA})_5$. The downfield signal was attributed to the $-\text{N}=\text{CH}_2-$ methylene groups, and the other two signals to the four $-\text{CH}_2-$ methylene groups of the diimine bridge. In fact, we did not detect the characteristic peak of the $-\text{CH}_2-\text{NH}_2$ methylene centred at $\approx 40\text{ ppm}$,¹⁹ which would indicate that HMDA was only attached by one of its amine groups. The presence of the diimine cross-linking molecule *N,N'*-(hexane-1,6-diyl)bis(1-imidazol-2-yl)methanimine) (Figure 4a) was finally confirmed by analysing the solution resulting from the digestion of $(\text{ZIF-90-HMDA})_5$ in acetic acid by $^1\text{H-NMR}$ and ESI-MS (Figure S66). The peaks at 8.58 ppm and 3.83 ppm in the $^1\text{H-NMR}$ spectrum were attributed to the $\text{CH}=\text{N}$ imine proton and the N-CH_2 methylene protons of the diamine molecule, respectively. On the other hand, in the ESI-MS spectra, the peak at $m/z = 273.1836$ matches with the molecular formula of the protonated *N,N'*-(hexane-1,6-diyl)bis(1-imidazol-2-yl)methanimine) $[\text{C}_{14}\text{H}_{20}\text{N}_6]^+$ ($m/z = 273.1822$).

$^1\text{H-NMR}$ spectrum of the digested $(\text{ZIF-90-HMDA})_5$ in strong acidic conditions (DCl , DMSO-d_6) was collected to quantify its yield of conversion (Figure S67). Comparison of the integration of the signals corresponding to ICA (7.56 ppm) and HMDA (1.30 ppm) revealed that there are 35% of HMDA, meaning that 70% of the ICA linkers were functionalized.

This high conversion of cross-linked ICA linkers in $(\text{ZIF-90-HMDA})_5$ should therefore involve a remarkable closure of its pores and reduction of its surface area in comparison to its parent ZIF-90. This assumption was confirmed by measuring the S_{BET} from the N_2 -sorption isotherm

“This document is the Accepted Manuscript version of a Published Work that appeared in final form in *Journal of the American Chemical Society*, copyright © American Chemical Society after peer review and technical editing by the publisher. To access the final edited and published work see: <https://doi.org/10.1021/jacs.6b11240>”

at 77 K. We found a S_{BET} of $69 \text{ m}^2 \text{ g}^{-1}$ that corresponds to a reduction of 93 % of the original S_{BET} of ZIF-90 (Table 2, Figures 4d and S68).

The contact angle (Θ_c) was also measured on a pressed pellet disk of (ZIF-90-HMDA)₅, giving a value of 110.9° , that correspond to a higher hydrophobic surface in comparison to the different (ZIF-90-BA)_x samples (Figures 4e).

CONCLUSION

We have reported a highly versatile and effective methodology to post-synthetically modify MOFs via Schiff-base condensation reactions. This strategy can be applied to MOFs with either terminal aldehyde or amine groups, reduces their PSM time, and enables their continuous PSM with good rates of conversion. Therefore, it should facilitate the PSM of MOFs for numerous applications, including catalysis, sensor technology, pollutant removal, and separation. This method also allowed the efficient crosslinking of the terminal aldehydes groups of ZIF-90 using a diamine molecule, thereby blocking their porosity and opening up new avenues for future triggered delivery systems. Finally, it also enables performing Schiff-base condensation reactions between discrete amine and aldehyde molecules, opening new perspectives in organic chemistry synthesis.

ASSOCIATED CONTENT

Supporting Information.

The following files are available free of charge.

Additional synthetic details, XRPD patterns, surface area measurements, FESEM images (PDF)

“This document is the Accepted Manuscript version of a Published Work that appeared in final form in *Journal of the American Chemical Society*, copyright © American Chemical Society after peer review and technical editing by the publisher. To access the final edited and published work see: <https://doi.org/10.1021/jacs.6b11240>”

AUTHOR INFORMATION

Corresponding Author

* E-mail: daniel.maspoch@icn2.cat

Notes

The authors have a patent pending on the methods described in this manuscript.

ACKNOWLEDGMENT

This work was supported by the EU FP7 ERC-Co 615954. I.I. thanks the MINECO for the RyC fellowship RyC-2010-06530. ICN2 acknowledges the support of the Spanish MINECO through the Severo Ochoa Centers of Excellence Program, under Grant SEV-2013-0295

REFERENCES

1. Furukawa, H.; Ko, N.; Go, Y. B.; Aratani, N.; Choi, S. B.; Choi, E.; Yazaydin, A. Ö.; Snurr, R. Q.; O’Keeffe, M.; Kim, J.; Yaghi, O. M. *Science* 2010, 329, 424.
2. Horcajada, P.; Gref, R.; Baati, T.; Allan, P. K.; Maurin, G.; Couvreur, P.; Ferey, G.; Morris, R. E.; Serre, C. *Chem. Rev.* 2012, 112, 1232.
3. Carné, A.; Carbonell, C.; Imaz, I.; Maspoch, D. *Chem. Soc. Rev.* 2011, 40, 291.
4. Evans, J. D.; Sumbly, C. J.; Doonan, C. J. *Chem. Soc. Rev.* 2014, 43, 5933.
5. Doonan, C. J.; Morris, W.; Furukawa, H.; Yaghi, O. M. *J. Am. Chem. Soc.* 2009, 131, 9492.
6. Kim, M.; Cahill, J. F.; Prather, K. A.; Cohen, S. M. *Chem. Commun.* 2011, 47, 7629.

“This document is the Accepted Manuscript version of a Published Work that appeared in final form in *Journal of the American Chemical Society*, copyright © American Chemical Society after peer review and technical editing by the publisher. To access the final edited and published work see: <https://doi.org/10.1021/jacs.6b11240>”

7. Garibay, S. J.; Cohen, S. M. *Chem. Commun.* 2010, 46, 7700.
8. Kim, M.; Cohen, S. M. *CrystEngComm* 2012, 14, 4096.
9. Kandiah, M.; Usseglio, S.; Svelle, S.; Olsbye, U.; Lillerud, K. P.; Tilset, M. J. *Mater. Chem.* 2010, 20, 9848.
10. Hou, J.; Luan, Y.; Tang, J.; Wensley, A. M.; Yang, M.; Lu, Y. J. *Mol. Catal. A: Chem.* 2015, 407, 53.
11. Pintado-Sierra, M.; Rasero-Almansa, A. M.; Corma, A.; Iglesias, M.; Sánchez, F. J. *Catal.* 2013, 299, 137.
12. Rasero-Almansa, A. M.; Corma, A.; Iglesias, M.; Sanchez, F. *Green Chem.* 2014, 16, 3522.
13. Tang, J.; Dong, W.; Wang, G.; Yao, Y.; Cai, L.; Liu, Y.; Zhao, X.; Xu, J.; Tan, L. *RSC Advances* 2014, 4, 42977.
14. Wang, J.; Yang, M.; Dong, W.; Jin, Z.; Tang, J.; Fan, S.; Lu, Y.; Wang, G. *Catal. Sci. Technol.* 2016, 6, 161.
15. Liu, J.; Zhang, X.; Yang, J.; Wang, L. *Appl. Organomet. Chem.* 2014, 28, 198.
16. Saleem, H.; Rafique, U.; Davies, R. P. *Microporous Mesoporous Mater.* 2016, 221, 238.
17. Morris, W.; Doonan, C. J.; Furukawa, H.; Banerjee, R.; Yaghi, O. M. *J. Am. Chem. Soc.* 2008, 130, 12626.
18. Jones, C. G.; Stavila, V.; Conroy, M. A.; Feng, P.; Slaughter, B.; Ashley, C. E.; Allendorf, M. D. *ACS Appl. Mater. Interfaces* 2016, 8, 7623.
19. Thompson, J. A.; Brunelli, N. A.; Lively, R. P.; Johnson, J. R.; Jones, C. W.; Nair, S. *J. Phys. Chem. C* 2013, 117, 8198.
20. Liu, C.; Liu, Q.; Huang, A. *Chem. Commun.* 2016, 52, 3400.

“This document is the Accepted Manuscript version of a Published Work that appeared in final form in *Journal of the American Chemical Society*, copyright © American Chemical Society after peer review and technical editing by the publisher. To access the final edited and published work see: <https://doi.org/10.1021/jacs.6b11240>”

21. Servalli, M.; Ranocchiari, M.; Van Bokhoven, J. A. *Chem. Commun.* 2012, 48, 1904.
22. Carné-Sánchez, A.; Imaz, I.; Cano-Sarabia, M.; Maspoch, D. *Nat Chem* 2013, 5, 203.
23. Garzon-Tovar, L.; Cano-Sarabia, M.; Carne-Sanchez, A.; Carbonell, C.; Imaz, I.; Maspoch, D. *React. Chem. Eng.* 2016, 1, 533.
24. Nguyen, J. G.; Cohen, S. M. *J. Am. Chem. Soc.* 2010, 132, 4560.
25. Canivet, J.; Aguado, S.; Daniel, C.; Farrusseng, D. *ChemCatChem* 2011, 3, 675.
26. Agudo, S.; Canivet, J.; Farrusseng, D. *Chem. Commun.* 2010, 46, 7999.
27. Marti, A. M.; Tran, D.; Balkus, K. J. *J. Porous Mater.* 2015, 22, 1275.
28. Ragon, F.; Horcajada, P.; Chevreau, H.; Hwang, Y. K.; Lee, U. H.; Miller, S. R.; Devic, T.; Chang, J.-S.; Serre, C. *Inorg. Chem.* 2014, 53, 2491.